

Milliwatt output levels and superquadratic bias dependence in a low-temperature-grown GaAs photomixer

E. R. Brown, K. A. McIntosh, F. W. Smith, K. B. Nichols, M. J. Manfra, C. L. Dennis, and J. P. Mattia

Lincoln Laboratory, Massachusetts Institute of Technology, Lexington, Massachusetts 02173-9108

(Received 2 September 1993; accepted for publication 6 April 1994)

A cw output power up to 0.8 mW is obtained from a low-temperature-grown (LTG) GaAs, 0.3 μm gap, interdigitated-electrode photomixer operating at room temperature and pumped by two modes of a $\text{Ti:Al}_2\text{O}_3$ laser separated in frequency by 0.2 GHz. The output power and associated optical-to-electrical conversion efficiency of 1% represent more than a sixfold increase over previous LTG-GaAs photomixer results obtained at room temperature. A separate LTG-GaAs photomixer having 0.6 μm gaps generated up to 0.1 mW at room temperature and up to 4 mW at 77 K. Low-temperature operation is beneficial because it reduces the possibility of thermal burnout and it accentuates a nearly quartic dependence of output power on bias voltage at high bias. The quartic dependence is explained by space-charge effects which result from the application of a very high electric field in the presence of recombination-limited transport. These conditions yield a photocurrent-voltage characteristic that is very similar in form to the well-known Mott-Gurney square-law current in trap-free solids.

Low-temperature-grown (LTG) GaAs remains of great interest to materials and device scientists alike because of its remarkable properties of high resistivity, high cross-gap photocarrier mobility relative to semiconductors of comparable resistivity, and very high dc breakdown fields. These properties have been utilized in several electrical and optical devices including field-effect transistors¹ and photon detectors.² Recently we have exploited these properties to make an optical heterodyne converter, or photomixer.³ In previous work, the output power and optical-to-electrical (O-E) conversion efficiency of a photomixer operating at room temperature were limited to 200 μW and 0.15%, respectively. Here, the performance is enhanced considerably by improving the interdigitated electrode structure and by operating the photomixer at cryogenic temperatures.

The LTG-GaAs material in the present experiment was grown by molecular beam epitaxy (MBE) on a semi-insulating GaAs substrate. The substrate temperature during growth was approximately 195 $^\circ\text{C}$ and the ratio of arsenic to gallium fluxes was set at 10:1. The LTG-GaAs epitaxial thickness was approximately 1.0 μm . After growth, the sample was annealed in the MBE chamber at a temperature of 600 $^\circ\text{C}$ for 10 min with an arsenic overpressure. The sample was then characterized by time-resolved photoreflectance and was found to have a photocarrier lifetime of approximately 0.2 ps.

After annealing, interdigitated electrodes were fabricated on the top surface of the LTG GaAs by electron-beam lithography to define the active region of the photomixer.³ The metal-electrode topography consisted of either forty 0.2- μm -wide electrodes separated by 0.3 μm gaps, or twenty 0.4- μm -wide electrodes separated by 0.6 μm gaps. The ratio of gap width to finger period in both structures is 20% higher than in our previous photomixer.³ In principle, this yields a 44% improvement in photomixer output power and O-E conversion efficiency from the increase in external quantum efficiency alone. The final step of the fabrication was the cre-

ation of an electrical coplanar waveguide structure around each set of interdigitated electrodes. The coplanar waveguide was defined by optical lithography and Ti/Au metal lift-off. The characteristic impedance of the coplanar waveguide was designed to be 50 Ω to facilitate the measurement of the photomixer output signal at microwave frequencies.

The photomixer was driven by a single (standing wave) $\text{Ti:Al}_2\text{O}_3$ solid-state laser operating at a wavelength near 750 nm. The laser was internally adjusted by etalons to operate with equal output power in two adjacent longitudinal modes separated in frequency by 200 MHz. The output beam was focused down to a spot diameter of approximately 20 μm at the photomixer active region and the total power was varied by changing the power of the argon-ion laser that pumped the $\text{Ti:Al}_2\text{O}_3$ crystal. For each pump power, the dc bias voltage was increased from zero up to a value just below that which produced catastrophic breakdown.

Shown in Fig. 1(a) are the experimental results for the 0.6 μm gap photomixer at room temperature and for total optical pump powers of 45 and 75 mW. At both power levels, we observed a nearly quadratic increase in output power with dc bias voltage up to about 8 V, followed by a superquadratic increase at higher voltages. At a fixed bias voltage less than about 5 V, the output power also increased quadratically with pump power between 45 and 75 mW. Both quadratic functions are characteristic of any photomixer in which the photocurrent depends linearly upon bias voltage. The superquadratic dependence on bias voltage is similar to that observed in previous experiments³ and is discussed below.

For 45 mW pump power, the output power at room temperature approaches a maximum value of -9 dBm at a bias voltage of 30 V. This represents an O-E conversion efficiency of approximately 0.3%. When the optical power or bias voltage was increased beyond this level, the device displayed thermal burnout. Burnout is not surprising under these operating conditions because the thermal conductivity of GaAs decreases rapidly with increasing temperature (ap-

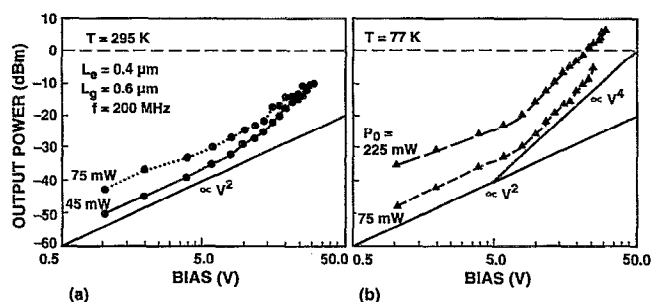


FIG. 1. Output power from 0.6 μm gap LTG-GaAs photomixer at 0.2 GHz as a function of bias voltage at two different operating temperatures: (a) $T=295 \text{ K}$, (b) $T=77 \text{ K}$. The dashed line in both figures denotes an output power of 0 dBm (1 mW).

proximately as $T^{-5/4}$ up to at least 500 °C. The resulting rapid increase of temperature with optical power causes the resistance of the LTG GaAs to drop significantly, which can cause the electrical current in the LTG GaAs to run away. In the present experiments, the photomixer was biased with a constant-voltage power supply so that current runaway could not be suppressed.

With burnout in mind, we tested a 0.6 μm gap photomixer at 77 K by mounting the coplanar-waveguide sample on the cold finger of a liquid-nitrogen crystal. The laser pump beam was focused on the photomixer through a glass window on the outer vacuum jacket of the cryostat. Shown in Fig. 1(b) are the experimental results for optical pump powers of 75 and 225 mW. For the 75 mW pump and bias voltages less than 10 V, the output power was slightly less than at room temperature with the same pump power. Above 10 V bias, the dependence on bias voltage became superquadratic, and the output power at 77 K exceeded that at room temperature. The output power for 225 mW pump power was nearly 10 times that obtained with 75 mW, power, consistent with the theoretical quadratic dependence of output power on pump power. Above 10-V bias, the output power increases in a nearly quartic fashion such that +6 dBm (4 mW) was obtained at 30 V bias. The highest O-E conversion efficiency at 77 K was 1.5% under the conditions of 225 mW pump power and 30 V bias.

Shown in Fig. 2 are the experimental results for the 0.3 μm gap photomixer operating at room temperature with optical pump powers of 30 and 85 mW. For 30 mW pump power, the output power is approximately quartic with bias voltage from 2 up to about 10 V. Beyond 10 V, the output power increases superquadratically in contrast to the behavior of the 0.6 μm gap device. With 85 mW pump power, the output power is quadratic up to about 5 V and then approximately quartic at higher voltages. The highest room-temperature output power was -1 dBm (0.8 mW), obtained with 85 mW pump power and 14 V bias. The highest O-E conversion efficiency was 1%, obtained with 30 mW pump power and 18 V bias. A bias of 18 V could not be applied with 85 mW pump power without destruction of the device, but a linear extrapolation of the curve in Fig. 2 yields a projected output power of +6 dBm (4 mW) under these conditions. We believe that this performance can be achieved

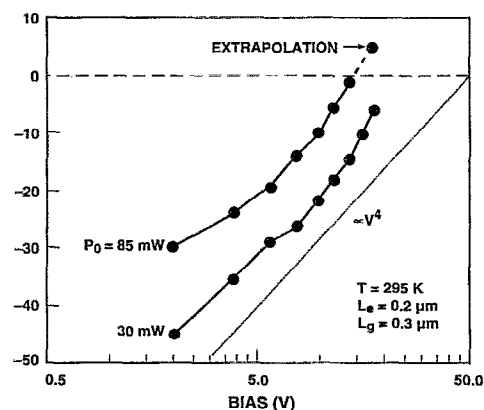


FIG. 2. Output power from 0.3 μm gap LTG-GaAs photomixer at 0.2 GHz as a function of bias voltage at room temperature. The horizontal dashed line denotes 1 mW. The dashed extrapolation to the curve for $P_0=85 \text{ mW}$ represents the projected output power of this device.

by better heat sinking of the device or, perhaps, simply by using a ballast resistor in the bias circuit.

To understand the physical characteristics of the photomixer, we have examined the dc photocurrent and dark current as functions of bias voltage under the same conditions as used above. Shown in Figs. 3(a) and 3(b) are the experimental results for the 0.6 μm gap device at room temperature and 77 K, respectively. Below 5 V bias, the photocurrent is linear for 45 mW pump power at room temperature, and for both pump powers at 77 K. The linear dependence in these samples is indicative of ohmic transport in the bulk LTG GaAs, and suggests that the bulk resistance limits the current through the device rather than the metal-to-LTG-GaAs contacts. It also explains the quadratic dependence of output power on bias voltage. According to optical-heterodyne theory, the output power at the difference frequency is given by $P_\omega = \langle i^2 \rangle Z_0$, where $\langle i^2 \rangle$ is the rms average of the ac photocurrent at the difference frequency and Z_0 is the characteristic impedance of the load circuit. For moderate optical pump powers, we can write this as $P_\omega = (1/2) S_I^2 P_1 P_2 Z_0$, where S_I is the external current responsivity, and P_1 and P_2 are the average powers of the two pump lasers. In the case of ohmic transport, $S_I \propto V$, so that $P_\omega \propto V^2$.

At bias voltages above 5 V in the 0.6 μm gap device and above 2 V in the 0.3 μm device, the photocurrent began to increase nearly quadratically. This is indicative of nonohmic transport in the LTG GaAs and it explains the onset of the quartic dependence of output power on bias through the same argument as given above. Because the range of bias voltage over which the superlinear photocurrent occurs is so broad and because this behavior has been observed in all of our LTG-GaAs photomixers measured to date, it becomes an essential factor in explaining the milliwatt-level output of these devices. We have carried out a qualitative analysis of the photocurrent based on the drift and current-continuity equations for electrons and holes, ignoring the effects of carrier diffusion. The electrons and holes were assumed to have the same recombination rate but different lifetimes, τ_e and τ_h , with $\tau_h > \tau_e$. The interdigitated electrodes were approximated as parallel plates with uniform current density be-

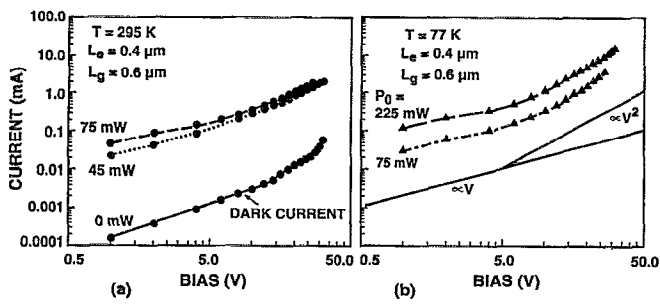


FIG. 3. Current-voltage curves for LTG-GaAs photomixer under the various experimental conditions: (a) $T=295$ K, (b) $T=77$ K. The dark-current curve at 77 K is not shown because it lies below the vertical current scale.

tween them. At low bias, ohmic behavior is displayed with the current density given by $J=e(n\mu_e+p\mu_h)E$, where $n(\mu_e)$ and $p(\mu_h)$ are the photoelectron and photohole densities (mobilities), respectively, and E is the electric field between the contacts. In the low bias limit, E is uniform and equal to V/L where L is the distance between electrodes in the parallel-plate approximation. When V is increased to the point where the quantity $L^2(\mu_e+\mu_h)/\mu_e\mu_hV$ becomes comparable to or less than $\tau_h-\tau_e$, the current density begins to increase quadratically consistent with the expression $J=(9/8)aV^2/L^3$ where $a=e(\mu_e\tau_e+\mu_h\tau_h)\mu_e\mu_hg(\tau_h-\tau_e)/(\mu_e+\mu_h)$ and g is the cross-gap photogeneration rate. For example, if we assume $L=0.6$ μm and the room-temperature values $\mu_e=400$ $\text{cm}^2\text{V}^{-1}\text{s}^{-1}$,⁵ $\mu_h\approx 100$ $\text{cm}^2\text{V}^{-1}\text{s}^{-1}$, $\tau_h\approx 5$ ps, $\tau_e\approx 0.2$ ps, we find a crossover from ohmic to quadratic behavior at $V\approx 16$ V. This is in good agreement with the photocurrent shown in Fig. 3(a).

The above quadratic current-voltage relation is very similar superficially to the Mott-Gurney law for a trap-free insulator in which the current is limited by the buildup of free space charge between the contacts.⁶ Our analysis for the LTG GaAs leads to a similar deviation from space-charge neutrality because of the difference between the electron and hole lifetimes and because of the high bias fields in the material which spatially separate the photogenerated electron-hole pairs. This deviation from ohmic behavior has conventionally been called "recombination-limited transport" and has been observed in semiconductors and insulators.⁷

Several other mechanisms have been considered to explain the superlinear behavior of the photocurrent. The first was cross-gap impact ionization. At the highest bias voltages, the electron potential-energy drop between the cathode and anode electrodes is over 10 times the GaAs band-gap energy E_g . This may enable photoelectrons generated near the cathode to gain the required kinetic energy, $3E_g/2$, to create a new electron-hole pair. However, when impact ionization occurs in semiconductor devices, it usually leads to avalanche breakdown, which is always characterized by a very rapid increase in current with voltage. Judging from the relatively gradual current-voltage characteristics in Fig. 3,

we believe that avalanche breakdown is not occurring in the 0.6 μm gap device. Nevertheless, we cannot rule out the possibility that either the small distance between electrodes or the very short recombination time in these samples is prohibiting avalanche multiplication but allowing for limited impact ionization. This may explain the superquadratic dependence at high bias voltages for the 0.3 μm device in Fig. 2.

A second mechanism that we considered was Zener tunneling at the As precipitates that exist in all LTG-GaAs samples annealed after the growth.⁸ We were led to this mechanism by an observation made long ago of soft reverse breakdown in Ge p - n diodes contaminated by metallic precipitates.⁹ We ruled out this mechanism based on the observed variation of the photocurrent with temperature. In comparing Figs. 3(a) and 3(b), we see that the quadratic dependence becomes much more pronounced in lowering the temperature to 77 K. In contrast, Zener tunneling in GaAs would become less pronounced because of the significant increase in E_g that occurs between room temperature and 77 K.¹⁰

In conclusion, we have demonstrated a LTG-GaAs photomixer having milliwatt output power levels in operation at room temperature and much greater output powers in operation at 77 K. The performance of this device is due in large part to a nearly quadratic dependence of photocurrent on bias voltage. We attribute the quadratic dependence to space-charge effects which result from the application of very high electric fields in the presence of recombination-limited transport. Because of the intrinsic photoconductive speed of the LTG GaAs, the milliwatt output power makes the photomixer very promising as a broadband tunable source operating from dc to frequencies well above 100 GHz.

We acknowledge K. M. Molvar, W. F. DiNatale, and D. J. Landers for expert technical assistance in the fabrication of photomixers, D. C. Look for helpful conversations and R. A. Murphy for useful comments on the manuscript. This research was sponsored by the Air Force Office of Scientific Research, the U.S. Army Research Office, and the Lincoln Laboratory Innovative Research Program.

¹F. W. Smith, *Mater. Res. Soc. Symp. Proc.* **241**, 1 (1992).

²Y. Chen, S. Williamson, T. Brock, F. W. Smith, and A. R. Calawa, *Appl. Phys. Lett.* **59**, 1984 (1991).

³E. R. Brown, K. A. McIntosh, F. W. Smith, M. J. Manfra, and C. L. Dennis, *Appl. Phys. Lett.* **62**, 1206 (1993).

⁴J. S. Blakemore, *J. Appl. Phys.* **53**, R123 (1982).

⁵D. C. Look, D. C. Walters, G. D. Robinson, J. R. Sizelove, M. G. Mier, and C. E. Stutz, *J. Appl. Phys.* **74**, 306 (1993).

⁶N. F. Mott and R. W. Gurney, *Electronic Processes in Ionic Crystals* (Oxford University Press, London, 1940).

⁷M. A. Lampert and P. Mark, *Current Injection in Solids* (Academic, New York, 1970).

⁸A. C. Warren, J. M. Woodall, J. H. Burroughes, P. D. Kirchner, H. K. Heinrich, G. Arjavalingam, N. Katzenellenbogen, D. Grischkowsky, M. R. Melloch, N. Otsuka, K. Mahalingam, F. H. Pollak, and X. Yin, *Mater. Res. Soc. Symp. Proc.* **241**, 15 (1992).

⁹A. Goetzberger and W. Shockley, *J. Appl. Phys.* **31**, 1821 (1960).

¹⁰S. Sze, *Physics of Semiconductor Devices* (Wiley, New York, 1982).